［溶接学会論文集　第 33 巻　第 2 号　p. 44s-48s（2015）］

Investigation of Droplet Ejection Mechanism from Electrode in Multi-Phase AC Arc*

by Taro Hashizume**, Manabu Tanaka*** and Takayuki Watanabe***

A multi-phase AC arc has various advantages such as high energy efficiency, large plasma volume and low gas velocity. Therefore, the multi-phase AC arc is suitable to massive powder processing like nanomaterial fabrication processes and innovative in-flight glass melting technology. However, the understanding of discharge behavior of multi-phase AC arc still remains to be improved for the practical use. In particular, electrode erosion is one of the most important issues to be solved. The purpose of this study is to investigate the droplet ejection mechanism of the multi-phase AC arc based on high-speed visualization by the high-speed camera and appropriate band-pass filters system. Obtained results indicated that droplet ejection was involved by variation in current and voltage during an AC cycle. The larger droplets were ejected at only cathodic period and the transition time from the cathodic to anodic AC period. Estimation of forces acting on the molten droplet revealed the electromagnetic force was most important force which leads to the detachment of the droplet from the electrode surface. Smaller droplet on the electrode tip leads to the droplet ejection due to the relatively stronger electromagnetic force than surface tension.

Key Words: Thermal plasmas, Multi-phase AC arc, Electrode erosion, Droplet ejection, High-speed visualization

1. Introduction

Thermal plasmas as an energy source with high energy efficiency have been applied in various engineering fields. They have various advantages such as extremely high temperature, high enthalpy to enhance reaction kinetics, rapid quenching capability to produce chemical non-equilibrium materials, and oxidation or reduction atmosphere in accordance with required chemical reaction. Therefore, thermal plasmas further attract notice recently[1)-3)].

The AC arc which is generated by AC power supply is one of the thermal plasmas. It has high energy efficiency because of the generation without converting AC to DC[4)-6)]. However, the existing single or three-phase AC arc have a characteristic of intermittent discharge due to the polarity transition. To improve the characteristic and obtain more effective reactor, a multi-phase AC arc was invented.

The multi-phase AC arc is generated among multi-electrodes with large plasma volume by phase-shifted AC power supplies. The multi-phase AC arc can be generated without the intermittent discharge because the arc always exists among 12 electrodes. Therefore it has various advantages such as high energy efficiency, large plasma volume, low gas velocity compared with the conventional thermal plasmas[7), 8)]. The multi-phase AC arc is expected to be applied to massive powder processing such as nanomaterial fabrication processes and innovative in-flight glass melting technology. However, fundamental phenomena in multi-phase AC arc have rarely been reported because of its novelty. In particular, electrode erosion is one of the most important issues to be solved because it determines the electrode lifetime and the purity of the products. Therefore, the purpose of the present study is to understand the droplet ejection mechanism by observation of the electrodes. High-speed video camera with appropriate band-pass filters system was applied to visualize electrode phenomena in the multi-phase AC arc. The dynamic behavior of metal droplet ejection from the electrode surface was observed.

*Received: 2014.11.28
**Dept. Chemical Systems and Engineering, Kyushu University
*** Dept. Chemical Engineering, Kyushu University

2. Experimental details

2.1 Experimental setup

Figure 1 shows a schematic image of experimental setup. It consisted of 12 electrodes, arc chamber, and AC power supply at 60Hz. The electrodes were made of tungsten (98wt%) and thoria (2wt%) with diameter of 3.2 mm or 6.0 mm. The electrodes were divided into two layers, upper six and lower six electrodes. Figure 2 shows a representative snapshot of multi-phase AC arc, which is taken from the top of the arc chamber. The electrodes were symmetrically arranged by the angle of 30 degree. To prevent the electrodes from oxidation, 99.99% argon was injected around the electrode as shield gas at 2-5 L/min of the flow rate. The applied voltage between each electrode and the neutral point of the coil of the transformer can be calculated by the following equation:

$$V_i = V_m \sin\left[\omega t - \frac{2\pi(i-1)}{12}\right] \quad (i = 1,2,...,12) \tag{1}$$

where V_i indicates the applied non-load voltage for each electrode number i and V_m indicates the amplitude of the non-load voltage (about 220 V, AC 60Hz). The arc current was changed from100 to 140 A for each electrode.

2.2 High-speed observation of electrode phenomena

Electrode phenomena in multi-phase AC arc were visualized by the high-speed camera system (FASTCAM SA-5, Photron Ltd., Japan). One of the electrodes was observed in the yellow frame by high-speed camera installed on the top of the arc generator as shown in Fig. 2. Observation of electrode during arc discharge was prevented by the strong emission of the arc. Therefore, the band-pass filters with 785 and 880 nm were combined with the high-speed camera system to separate the electrode thermal radiation from the emission of the arc. The clear visualization of electrode tip was achieved by the combination of high-speed camera and band-pass filters.

2.3 Temperature measurements of electrode surface

The electrode surface temperature was also measured by the same camera systems mentioned above. Based on two-color pyrometry, following equation was applied to calculate the surface temperature:

$$T = \frac{hc(\lambda_1 - \lambda_2)}{k\lambda_1\lambda_2}\left[\ln R + 5\ln\left(\frac{\lambda_1}{\lambda_2}\right)\right]^{-1} \quad (2)$$

h is Planck constant, c is speed of light and k is Boltzmann constant. Temperature T is estimated from the ratio of thermal radiation intensities R at different wavelengths λ_1 and λ_2.

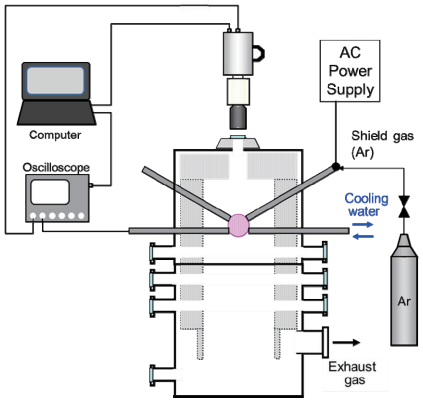

Fig. 1 Schematic image of multi-phase AC arc generator.

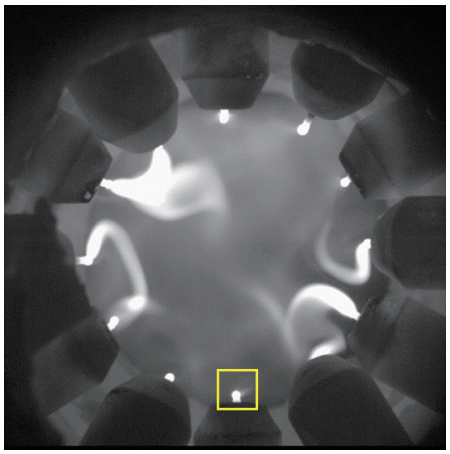

Fig. 2 Representative snapshot of multi-phase AC arc.

3. Result and discussion

3.1 Droplet ejection during an AC cycle

High-speed camera observation revealed that the diameters of droplets ejected from the electrodes were distributed in the range from tens to several hundred micrometers. Figure 3 (a) shows representative snapshots of the large droplet ejection from 6.0 mm diameter electrode during the cathodic period and Fig. 3 (b) shows voltage waveforms synchronized with the high-speed camera. The electrode tip in molten state became hemispherical shape. The droplet then detached from the electrode surface as in Fig. 3 (a).

Figure 4 (a) shows representative snapshots of 6.0 mm diameter electrode during the anodic period and Fig. 4 (b) shows voltage waveforms. As well as the cathodic period, the electrode tip became hemispherical shape forming a droplet. However the droplet became small returning to the electrode without detachment from the electrode tip. The reason for this different behavior will be discussed in following section.

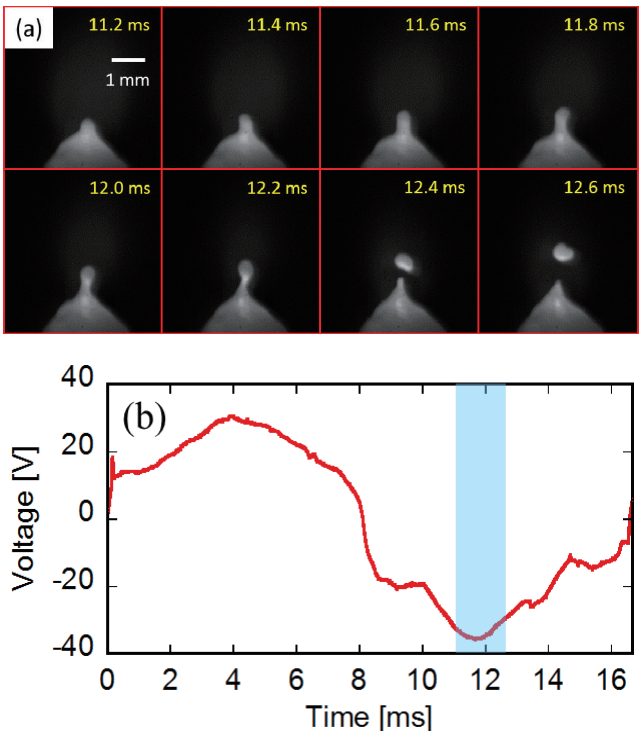

Fig. 3 Representative snapshots of molten electrode tip observed at cathodic period (a) and synchronized voltage waveform (b).

Figure 5 shows time transient of the number of the ejected droplets during AC cycles. At the first half period, the electrode is in the anodic period whereas the second half corresponds to the cathodic period. Red plots with solid line indicate the total number of droplets ejected from 6.0 mm diameter electrode. Three peaks can be found at anodic period, cathodic period, and the transition time from the cathodic to anodic period. On the other hand, the blue plots with broken line in Fig. 5 indicate the number of the droplets larger than 250 μm in diameter. Only two peaks are found at the cathodic period and at the transition time from the cathodic to the anodic period. This result suggests that the electrode erosion by droplet ejection mainly occurred at cathodic period and the transition time from the cathodic to anodic period.

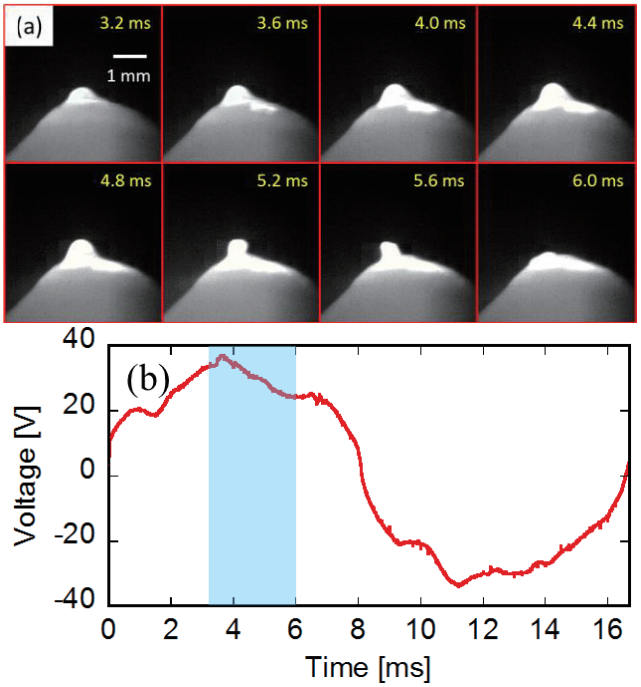

Fig. 4 Representative snapshots of molten electrode tip observed at anodic period (a) and synchronized voltage waveform (b).

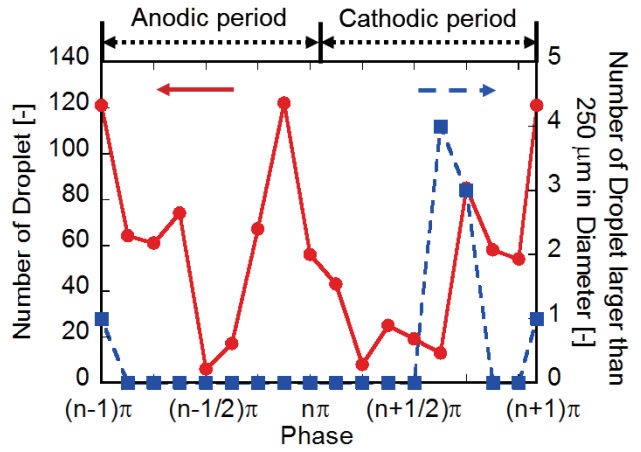

Fig. 5 Time transient of the number of the ejected droplets during AC periods at 60 Hz.

3.2 Electrode erosion with different electrode diameters

Figure 6 (a) shows representative snapshots of 3.2 mm diameter electrode during an AC cycle and Fig. 6 (b) shows voltage waveforms synchronized with the high-speed camera. The whole of the tip of 3.2 mm diameter electrode was melted, and the molten tip diameter was larger than the electrode diameter. Contrasting to the 6.0 mm diameter electrode, the droplet in the case of 3.2 mm rarely detached from the electrode surface. This difference will also be discussed in the following section with the consideration of the forces acting on the molten droplets.

Figure 7 shows electrode erosion rate with different electrode diameters. Red bar indicates the erosion rate by evaporation and

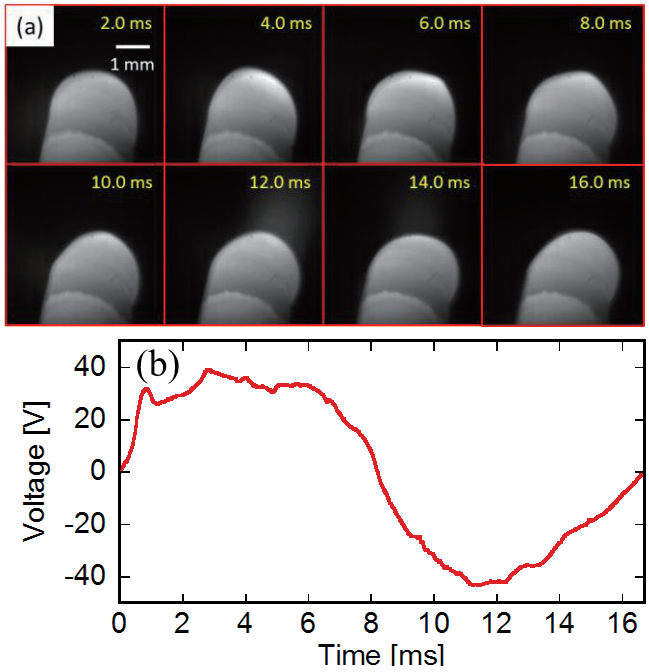

Fig. 6 Representative snapshots of molten tip of 3.2 mm diameter electrode during an AC cycle (a) and synchronized voltage waveforms (b).

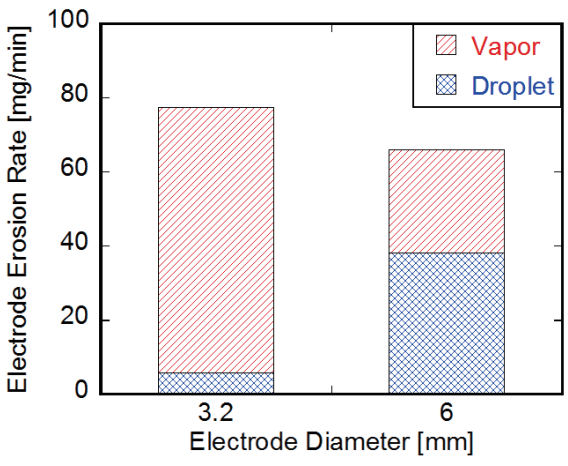

Fig. 7 Electrode erosion rate with different electrode diameters.

blue bar indicates that by droplet ejection. Total erosion rate of 3.2 mm diameter electrode was larger than that of 6.0 mm diameter electrode even though the droplet ejection rate of 3.2 mm diameter electrode was much lower than that of 6.0 mm diameter electrode. This can be explained by the different erosion mechanism. Smaller electrode diameter leads to the lower cooling efficiency, resulting in the higher surface temperature leading to higher evaporation rate. Consequently, the electrode erosion mechanism changed with different electrode diameter.

3.3 Force balance on the molten electrode

Ejection of large droplets from 6.0 mm diameter electrode occurred at only cathodic period. Moreover, droplets were rarely ejected from 3.2 mm diameter electrode. The mechanism of the ejection of larger droplets is investigated by the evaluation of forces on droplets. Evaluations of the major forces acting on the molten tip are given in the following.

The forces due to the surface tension, P_{st}, which pulls the electrode tip in molten state back is considered as in Eq. (3).

$$P_{st} = \frac{\sigma}{r} \tag{3}$$

where σ is the surface tension and r is the radius of the electrode tip in molten state.

The electromagnetic force, P_{em}, is caused by interaction of current flowing inside electrode tip with the self-induced magnetic field in the azimuthal direction. With the assumption that the axial current density is distributed uniformly over any horizontal cross section of the droplet, the electromagnetic force is given by:

$$P_{em} = \frac{\mu_0}{8\pi}\frac{I^2}{r^2} \tag{4}$$

where μ_0 is magnetic permeability and I is the total arc current.

The pressure due to ion attack on the electrode surface should be considered at the cathodic period because the ion with positive charge is accelerated towards the electrode only at the cathodic period. The number of ions impacting the cathode per unit area and per unit time is:

$$n = \frac{\eta j}{e} \tag{5}$$

where j is the current density and e is the electron charge. η is the current fraction of the total current. j is estimated by Richardson-Dushman formula:

$$j = AT^2 \exp\left(-\frac{\phi}{kT}\right) \tag{6}$$

A is Richardson constant and ϕ is work function of tungsten. j is estimated from electrode temperature T estimated by Eq. (2). The pressure is equal to the momentum change of these impacting ions:

$$P_{ion} = \eta j\sqrt{\frac{2m_i V}{e}} \tag{7}$$

where m_i is the ion mass and V is the sheath voltage at the cathode. V is assumed to be 10 V. In the present evaluation, the ion current fraction was assumed to be 30 %, which is reasonable value reported in the previous studies about the electrode phenomena in DC arc torches with thoriated-tungsten cathode[9].

Surface tension and ion pressure are the forces which pull the droplet back to the electrode side, resulting in suppress of droplet ejection. On the other hand, the electromagnetic force is the force squeezes and detaches the droplet from the electrode, resulting in the droplet ejection.

The evaluated forces for the electrodes in different periods and diameters are summarized in Fig. 8. Figure 8 (a) shows a schematic image of the major forces acting on the tip of 6.0 mm diameter electrode at cathodic period. The result shows that the dominant force at the cathodic period in 6.0 mm diameter electrode is the electromagnetic force. In contrast, the dominant force at the anodic period in 6.0 mm diameter electrode is the surface tension, as shown in Fig. 8 (b). This difference can be explained by the different size of the droplet on the electrode. The electrode tip was partially melted due to the heat transfer from the arc. The heat transfer at the anodic period is larger than that at the cathodic period. Thus, the volume of the molten part at the anodic

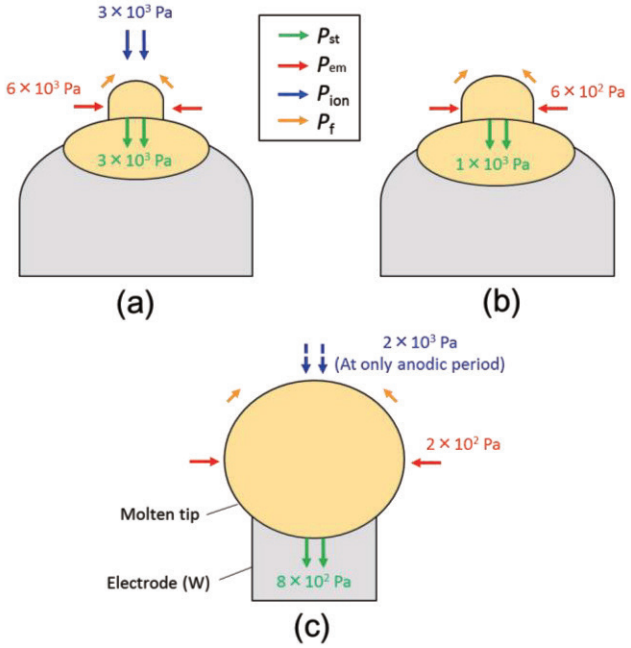

Fig. 8 Schematic image of the force balance on 6.0 mm diameter electrode at cathodic period (a), at anodic period (b), and on 3.2 mm diameter electrode (c).

period is larger than that at the cathodic period, resulting in the larger hemispherical droplet on the electrode at the anodic period. As shown in Eqs. (3) and (4), the surface tension and the electromagnetic force are proportional to r^{-1} and r^{-2}, respectively, where r is the radius of the droplet. Therefore, the electromagnetic force at the cathodic period became more important than the surface tension, whereas the surface tension was dominant at the anodic period. From the evaluation of the major forces on the molten tip, the electromagnetic force mainly causes ejection of larger droplets.

Figure 8 (c) shows a schematic image of the major forces acting on the tip of 3.2 mm diameter electrode. The droplet size on 3.2 mm diameter electrode was much larger than that on 6.0 mm diameter electrode. Therefore, the electromagnetic force causing ejection of larger droplets was weak and the surface tension was dominant, resulting in the negligible droplet ejection.

Above discussion in the previous paragraphs suggest that the droplet size on the electrode surface has important role to determine whether the droplet finally detaches from the electrode surface or not. In case of the larger droplet, the droplet ejection is negligible. Therefore, the smaller electrode diameter with larger droplet on the electrode surface is effective to prevent the droplet ejection. However, as shown in Fig. 7, the electrode erosion by evaporation in the case of the smaller electrode diameter drastically increases due to lower cooling efficiency. The optimization of the electrode diameter is necessary in accordance with the total erosion by both droplet ejection and the metal evaporation.

The droplet ejection mechanism was investigated by the high-speed visualization of the electrode phenomena in the multi-phase AC arc. The correlation between the experimental results and the evaluated results of the forces acting on the droplet suggests that the droplet size is one of the most important parameter to determine the droplet ejection. The dynamic behavior of the droplet has not been discussed yet. Time evolution of the forces acting on the droplet must be important and currently under investigation.

4. Conclusions

The dynamic behavior of droplets ejection was successfully visualized by the high-speed camera observation combined with the appropriate band-pass filters system. The effect of the electrode diameter and the polarity on the droplet ejection was investigated. Results indicated that the electrode erosion by the droplet ejection is mainly attributed to the droplets with diameter larger than 250 μm at the cathodic period and at the transition time from the cathodic to anodic period. According to the evaluation of the forces acting on the molten electrode, the droplet size is important parameter to determine the dominant force. Smaller droplet on the electrode tip leads to detachment of the droplet from the electrode surface due to the relatively stronger electromagnetic force than surface tension. On the other hand, the larger droplet leads to the negligible droplet ejection due to the relatively stronger surface tension than the electromagnetic force. Understanding the erosion mechanism and decreasing the erosion rate enable to realize the practical use of the multi-phase AC arc in various applications.

Reference

1) T. Watanabe, Narengerile, and H. Nishioka: Role of CH, CH_3, and OH Radicals in Organic Compound Decomposition by Water Plasmas, Plasma Chem. Plasma Process. 32 (2011) 123.
2) M. Shigeta and T. Watanabe: Growth mechanism of silicon-based functional nanoparticles fabricated by inductively coupled thermal plasmas, J. Phys. D: Appl. Phys. 40 (2007) 2407.
3) M. Tanaka and T. Watanabe: Mechanism of Enhanced Vaporization from Molten Metal Surface by Argon-Hydrogen Arc Plasma, Jpn. J. Appl. Phys, 52 (2013) 076201.
4) J.E. Harry, R. Knight: Simultaneous operation of electric arcs from the same supply, IEEE Trans. Plasma Sci. 9 (1981) 248.
5) J.E. Harry, R. Knight: Investigation of the intensity distribution of large volume multiple-arc discharges, J. Phys. D: Appl Phys. 17 (1984) 343.
6) T. Watanabe, K. Yasuda, T. Yano, T. Matsuura: Innovative in-flight glass-melting technology using thermal plasmas, Pure Appl. Chem. 82 (2010) 1337.
7) Y. Yao, T. Watanabe, T. Yano, T. Iseda, O. Sakamoto, M. Iwamoto, and S. Inoue: An innovative energy-saving in-flight melting technology and its application to glass production, Sci. Technol. Adv. Mat. 9 (2008) 8.
8) Y. Yao, K. Yasuda, T. Watanabe, F. Funabiki, and T. Yano: Investigation on in-flight melting behavior of granulated alkali-free glass raw material under different conditions with 12-phase AC arc, Chem. Eng. J. 144 (2008) 317.
9) X. Zhou and J. Heberlein: Analysis of the arc cathode interaction of free-burning arcs, Plasma Sources Sci. Technol. 3 (1994) 564.